

Vacuum-induced coherence in quantum dot systems

Anna Sitek* and Paweł Machnikowski†

Institute of Physics, Wrocław University of Technology, 50-370 Wrocław, Poland

We present a theoretical study of vacuum-induced coherence in a pair of vertically stacked semiconductor quantum dots. The process consists in a coherent excitation transfer from a single-exciton state localized in one dot to a delocalized state in which the exciton occupation gets trapped. We study the influence of the factors characteristic of quantum dot systems (as opposed to natural atoms): energy mismatch, coupling between the single exciton states localized in different dots, different and non-parallel dipoles due to subband mixing, as well as coupling to phonons. We show that the destructive effect of the energy mismatch can be overcome by an appropriate interplay of the dipole moments and coupling between the dots which allows one to observe the trapping effect even in a structure with technologically realistic energy splitting on the order of milli-electron-Volts. We also analyze the impact of phonon dynamics on the occupation trapping and show that phonon effects are suppressed in a certain range of system parameters. This analysis shows that the vacuum induced coherence effect and the associated long-living trapped excitonic population can be achieved in quantum dots.

PACS numbers: 78.67.Hc, 78.47.Cd, 03.65.Yz

I. INTRODUCTION

Pairs of closely stacked quantum dots (QDs) coupled via inter-band dipole moments^{1,2} (double quantum dots, DQDs) or by tunneling resulting from carrier wave function overlap and Coulomb correlations³⁻⁶ (quantum dot molecules, QDMs) attract much attention due to the richness of their physical properties which show huge technological promise for nanoelectronics, spintronics and quantum information processing applications. The unique features of these systems, as compared to individual QDs, can be used as the basis for long-time storage of quantum information⁷ and conditional optical control of carrier states⁸ which pave the way to an implementation of a two-qubit quantum gate⁹. Double dot structures enable also coherent optical spin control and entangling¹⁰⁻¹² or may act as sources of entangled photons¹³. It has been shown that the exciton spectrum of a QDM can be used to define an excitonic qubit with an extended life time¹⁴, that information can be written on the spin state of the dopant Mn ion located in one of the dots forming a DQD¹⁵, and that a photon emitted by a nearby quantum point contact may induce carrier transfer in a DQD system¹⁶. The richness and complexity of the physical properties of these systems have been manifested in many optical experiments¹⁷⁻¹⁹.

The spacing between the dots forming intentionally manufactured DQDs and QDMs is typically on the order of nanometers which is two to three orders of magnitude smaller than the wavelength of a resonantly coupled photon. Under such conditions, in atomic samples the effect of superradiant emission is observed²⁰. A similar effect of coupling to common radiative modes appears also in the emission from QD systems. Here also superradiance-like phenomena occur in the evolution of the exciton occupation and polarization.²¹⁻²⁴ Apart from the modified evolution for spontaneous emission, collective coupling to the radiation field can lead to other physical effects,

one of which is the vacuum induced coherence (VIC)²⁵. This effect consists in spontaneous, partial coherent excitation transfer from an initially occupied QD to initially empty one which results in exciton occupation trapping in a decoherence-resistant state. Like the superradiance phenomena, the VIC effect can be expected to occur also in QD systems.

On the other hand, although natural atoms and QDs have many properties in common, the characteristic feature of the latter is the inhomogeneity of transition energy which, for technologically realistic structures, is on the order of milli-electron-Volts. Moreover, small spatial separation of the dots leads to coupling between them²⁶. In our previous works we studied the impact of the transition energy mismatch and the coupling between the two emitters on the stability of collective effects^{27,28} and their role in the linear²⁹ and nonlinear optical response of the DQD systems³⁰. We showed that, in the absence of coupling between the QDs, the appearance of an optically inactive subradiant state and a rapidly decaying superradiant one are extremely sensitive to the fundamental transition energy mismatch and already for a mismatch on the order of micro-electron-Volts the collective character of the evolution is replaced by oscillation around the average exponential decay. The destructive effect of the system inhomogeneity may be, to some extent, overcome by sufficiently strong coupling between the dots which rebuilds collective behavior even in structures with technologically realistic values of energy mismatch^{22,28}. We have also pointed out that phonon-induced dynamics can slow down the decay of a superradiant state or speed up the emission from the superradiant one³¹. Based on these previous investigations of superradiance phenomena in QDs, one can expect that the VIC effect should, in principle, also be observable in these systems, at least in the presence of sufficiently strong coupling²⁷. However, to our knowledge, its stability against various inhomogeneities and perturbations

typical for the solid state environment (in particular non-parallel orientation of the interband dipoles in the two dots as well as phonon perturbations) have not been studied.

In this paper, we study the necessary conditions for the VIC effect to appear in a system of two vertically stacked semiconductor QDs. We investigate the role of the fundamental transition energy mismatch, coupling between the dots, and phonon-induced kinetics in this process. We also pay particular attention to the difference of the magnitude of the interband dipole moments as well as to their non-parallel alignment (due to sub-band mixing). We show that in spite of all these inhomogeneities that are typical to QD structures (as opposed to natural atoms) the vacuum-induced coherence can be almost fully stabilized in realistic pairs of non-identical QDs in a certain range of parameters. In particular, different interband dipole moments for the two dots lead to the appearance of a state which is perfectly immune to radiative decay for a particular choice of the system parameters.

The paper is organized as follows. In Sec. II, we describe the system under investigation and define its model. In Sec. III, the method for describing the evolution is described. Section IV contains the discussion of the results. Concluding remarks are contained in Section V.

II. THE SYSTEM

The investigated system is composed of two vertically stacked semiconductor QDs interacting with quantum electromagnetic field and lattice vibrations. We restrict the discussion to the ground-level transitions with fixed polarization and spin orientations. We take into consideration only ‘spatially direct’ states in which electron-hole pairs reside in the same QD. Due to the strong Coulomb coupling these states have a much lower energy than the ‘dissociated’ states (the external electric fields which would change this picture^{6,32} are not considered in our discussion). In this manner, the DQD or QDM may be described as a four-level system, with the state $|00\rangle$ denoting empty dots, states $|10\rangle$ and $|01\rangle$ representing single-exciton states with electron-hole pairs residing in the lower or higher QD, and the $|11\rangle$ corresponding to the biexciton state, that is, to both QDs occupied with an exciton.

As it is currently impossible to produce on demand pairs of QDs with identical fundamental transition energies, we assume that the exciton transition energies for the two dots are different,

$$E_1 = E + \Delta \quad \text{and} \quad E_2 = E - \Delta,$$

where E is the average transition energy and Δ is the energy mismatch.

As in Ref. 29, we describe the evolution in the ‘rotating

basis’ defined by the unitary transformation

$$U = e^{-i[E(|10\rangle\langle 10| + |01\rangle\langle 01| + 2|11\rangle\langle 11|) + H_{\text{rad}} + H_{\text{ph}}]t/\hbar},$$

where H_{rad} and H_{ph} are the standard free photon and phonon Hamiltonians, respectively. The Hamiltonian of the system is then

$$H = H_{\text{DQD}} + H_{\text{DQD-ph}} + H_{\text{DQD-rad}}. \quad (1)$$

The first term describes exciton states in a DQD structure.

$$H_{\text{DQD}} = \Delta(|10\rangle\langle 10| - |01\rangle\langle 01|) + V_{\text{B}}|11\rangle\langle 11| + V(|10\rangle\langle 01| + |01\rangle\langle 10|), \quad (2)$$

where V_{B} is a biexciton shift due to the interaction of static dipole moments and V is the amplitude of the coupling between the single-exciton states of the dots.

The QDs are separated by a distance on the order of a few nm which is much smaller than the relevant wave length of the electromagnetic field with which the dots interact. This allows us to neglect the space dependence of the electromagnetic field and describe the coupling of excitons to the photon modes in the Dicke limit²⁰. The relevant Hamiltonian in the dipole and rotating wave approximations is then

$$H_{\text{DQD-rad}} = \sum_{\alpha=1}^2 \sum_{\mathbf{k}\lambda} \sigma_{\mathbf{k}\lambda}^{\alpha} g_{\mathbf{k}\lambda}^{\alpha} e^{-i(\frac{E}{\hbar} - \omega_{\mathbf{k}})t} b_{\mathbf{k},\lambda}^{\dagger} + \text{H.c.}$$

where $\sigma_{\pm}^{\alpha} = (\sigma_{\mp}^{\alpha})^{\dagger}$ are the creation and annihilation operators for the exciton in the α th QD, $b_{\mathbf{k}}^{\dagger}$ is the creation operator of the photon mode with the wave vector \mathbf{k} , and

$$g_{\mathbf{k}\lambda}^{\alpha} = i\mathbf{d}_{\alpha} \cdot \hat{\mathbf{e}}_{\lambda}(\mathbf{k}) \sqrt{\frac{\hbar\omega_{\mathbf{k}}}{2\epsilon_0\epsilon_r v}}$$

is a coupling constant for the α th QD, where \mathbf{d}_{α} is the inter-band dipole moment for the α th QD, $\hat{\mathbf{e}}_{\lambda}(\mathbf{k})$ is the unit polarization vector of the photon mode with polarization λ , $\omega_{\mathbf{k}}$ is the corresponding frequency, ϵ_0 is the vacuum dielectric constant, ϵ_r is the relative dielectric constant of the semiconductor and v is the normalization volume. We investigate only wide-gap semiconductors with fundamental transition energies on the order of 1 eV for which zero-temperature approximation for the electromagnetic modes may be used at any reasonable temperature.

Interaction of the carriers confined in the two dots with phonon modes is modeled by the Hamiltonian

$$H_{\text{DQD-ph}} = \sum_{\alpha=1,2} \sigma_{+}^{\alpha} \sigma_{-}^{\alpha} \sum_{\mathbf{q}} f_{\mathbf{q}}^{(\alpha)} (c_{\mathbf{q}} + c_{-\mathbf{q}}^{\dagger}),$$

where $c_{\mathbf{q}}^{\dagger}$ and $c_{\mathbf{q}}$ are creation and annihilation operators of the phonon mode with the wave vector \mathbf{q} and $f_{\mathbf{q}}^{(1,2)}$ are the system reservoir coupling constants for the first and second QD, respectively. We model the electron and hole

wave functions by identical Gaussians with extensions l in the xy plane and l_z along the growth direction,

$$\Psi(\mathbf{r}) \sim \exp\left(-\frac{1}{2}\frac{x^2+y^2}{l^2} - \frac{1}{2}\frac{z^2}{l_z^2}\right).$$

For such wave functions and for the deformation potential couplings between the confined carriers and longitudinal phonon modes, the coupling constants have the form³¹

$$f_{\mathbf{q}}^{(1,2)} = f_{\mathbf{q}} \exp\left[\pm \frac{iq_z D}{2}\right],$$

where D is the distance between the dots and

$$f_{\mathbf{q}} = (\sigma_e - \sigma_h) \sqrt{\frac{\hbar q}{2\rho v c_l}} \exp\left[-\frac{l_z^2 q_z^2 + l^2 q_{\perp}^2}{4}\right].$$

Here $\sigma_{e/h}$ are deformation potential constants for electrons/holes, ρ is the crystal density, c_l is the speed of longitudinal sound (linear phonon dispersion is assumed) and $q_{\perp, z}$ are momentum components in the xy plane and along the z axis.

III. THE EVOLUTION

Analytical formulas describing the evolution of a pair of QDs are available for uncoupled systems ($V = 0$) interacting only with phonon modes³³ and, in the Markov limit, if only radiative decay is included²⁸. In this paper we use the previously proposed method³⁴ that allows us to deal with the simultaneous action of both the phonon and photon surroundings. Our approach is based on the equation of motion for the reduced density matrix of the carrier subsystem in the interaction picture,

$$\dot{\rho} = \mathcal{L}_{\text{rad}}[\rho] + \mathcal{L}_{\text{ph}}[\rho]. \quad (3)$$

Here the first term accounts for the effects induced by the radiative environment, which is described in the Markov limit by the Lindblad dissipator

$$\mathcal{L}_{\text{rad}}[\rho] = \sum_{\alpha\beta=1}^2 \Gamma_{\alpha\beta} \left[\sigma_{-}^{\alpha}(t) \rho \sigma_{+}^{\beta}(t) - \frac{1}{2} \left\{ \sigma_{+}^{\beta}(t) \sigma_{-}^{\alpha}(t), \rho \right\} \right], \quad (4)$$

where

$$\sigma_{-}^{\alpha}(t) = [\sigma_{+}^{\alpha}(t)]^{\dagger} = \exp\left[\frac{iH_{\text{DQD}}t}{\hbar}\right] \sigma_{-}^{\alpha} \exp\left[-\frac{iH_{\text{DQD}}t}{\hbar}\right]$$

and

$$\Gamma_{\alpha\beta} = \Gamma_{\beta\alpha}^{*} = \frac{E^3}{3\pi\epsilon_0\epsilon_r\hbar^4} \mathbf{d}_{\alpha} \cdot \mathbf{d}_{\beta}^{*}. \quad (5)$$

If we assume that the spontaneous decay rates for the two QDs are Γ_{11} and Γ_{22} then it follows directly from Eq. (5) that

$$\Gamma_{12} = \Gamma_{21}^{*} = \sqrt{\Gamma_{11}\Gamma_{22}} \hat{\mathbf{d}}_1 \cdot \hat{\mathbf{d}}_2^{*},$$

Parameter	Symbol	Value
Difference of deformation potential		
constants for electrons and holes	$\sigma_e - \sigma_h$	9 meV
Crystal density	ϱ	5350 kg/m ³
Speed of longitudinal sound	c_l	5150 m/s
Carrier localization extensions		
in the xy plane	l	4.5 nm
Carrier localization extensions		
in the growth direction	l_z	1 nm
Spatial separation of the dots	D	8 nm

TABLE I. Parameters used in numerical simulations. The values correspond to a self-assembled InAs/GaAs system.

where $\hat{\mathbf{d}}_{\alpha} = \mathbf{d}_{\alpha}/d_{\alpha}$. By redefining the relative phase of the exciton states in the two dots one can assume without any loss of generality that Γ_{12} and Γ_{21} are real.

The second term in Eq. (3) accounts for the effects due to interaction with phonon surrounding, allowing for non-Markovian dynamics. To describe these effects we use the time-convolutionless equation

$$\mathcal{L}_{\text{ph}}[\rho] = - \int_0^t d\tau \text{Tr}_{\text{ph}}[H_{\text{DQD-ph}}(t), [H_{\text{DQD-ph}}(\tau), \rho(t) \otimes \rho_{\text{ph}}]],$$

where

$$H_{\text{DQD-ph}}(t) = \exp\left[\frac{iH_{\text{DQD}}t}{\hbar}\right] H_{\text{DQD-ph}} \exp\left[-\frac{iH_{\text{DQD}}t}{\hbar}\right],$$

ρ_{ph} is the phonon density matrix at thermal equilibrium, and Tr_{ph} denotes partial trace with respect to the phonon degrees of freedom.

IV. RESULTS AND DISCUSSION

Below, we present our results of simulations of the VIC process in pairs of QDs. In all the analyzed cases, we assume that the system is prepared initially in a localized state $|10\rangle$. In Sec. refs:subsec:identical we explain the effect in a system of identical, uncoupled dots. Then, in Sec. IV B, we analyze the role of the relative magnitude and orientation dipole moments and in Sec. IV C the effect of the energy mismatch and coupling between the dots. In Sec. IV D we analyze the interplay of all the parameters that distinguish QDs from natural atoms in the evolution of QDs interacting only with radiation reservoir. The phonon impact on the VIC is discussed in Sec. IV E.

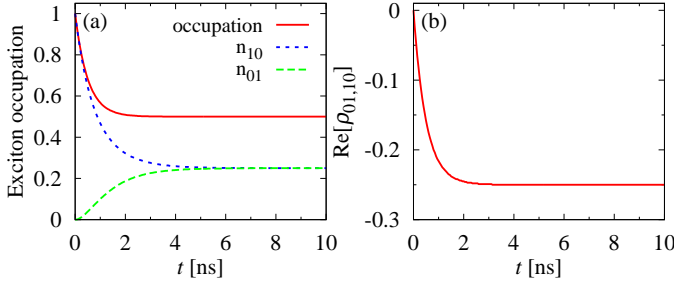


FIG. 1. (Color online) Vacuum-induced coherence in a system of two identical ($\Delta = 0$, $\Gamma_{11} = \Gamma_{22} = 1 \text{ ns}^{-1}$) two-level systems. (a) Exciton occupation of the system and occupations of the states $|10\rangle$ (n_{10}) and $|01\rangle$ (n_{01}). (b) The off-diagonal density matrix element $\rho_{01,10}$.

A. Identical QDs

Collective coupling of two identical QDs (systems with identical fundamental transition energies and parallel dipole moments of equal magnitudes) to the quantum electromagnetic vacuum leads to the appearance of a short-living (bright) superradiant state, $|+\rangle = (|10\rangle + |01\rangle)/\sqrt{2}$, and an optically inactive (dark) subradiant state $|-\rangle = (|10\rangle - |01\rangle)/\sqrt{2}$. The initial state of the analyzed system is a localized single-exciton state ($|10\rangle$ or $|01\rangle$) which can appear naturally, e.g., as an effect of incoherent trapping or controlled tunnel injection of carriers in an injection structure similar to that studied in Ref. 35. Such a state of a system of two identical and uncoupled QDs may be expressed as an equal combination of the sub- and superradiant states, $|-\rangle$ and $|+\rangle$,

$$|10\rangle = \frac{1}{\sqrt{2}}(|+\rangle + |-\rangle), \quad |01\rangle = \frac{1}{\sqrt{2}}(|+\rangle - |-\rangle). \quad (6)$$

Coupling to the electromagnetic reservoir induces emission from the bright state and, consequently, decay of a half of the initial excitation, while the other half is unaffected (trapped) due to the stability of the subradiant state for a system of two identical two-level systems²⁸. This is observed as a spontaneous and coherent excitation transfer from initially occupied dot to the initially empty one until occupation of both QDs stabilizes at the same level (Fig. 1a). While this process is taking place, coherence builds up spontaneously in the system (Fig. 1b). As a consequence, the pair of identical QDs is trapped in a delocalized and decoherence-resistant state with the exciton occupation number equal 0.5 and real off-diagonal matrix element equal -0.25 . This effect is referred to as VIC.

B. The role of dipole moments

Vertically stacked semiconductor QDs differ slightly in size and shape. If the system was formed in a self-assembled two-layer process then the upper QD is usu-

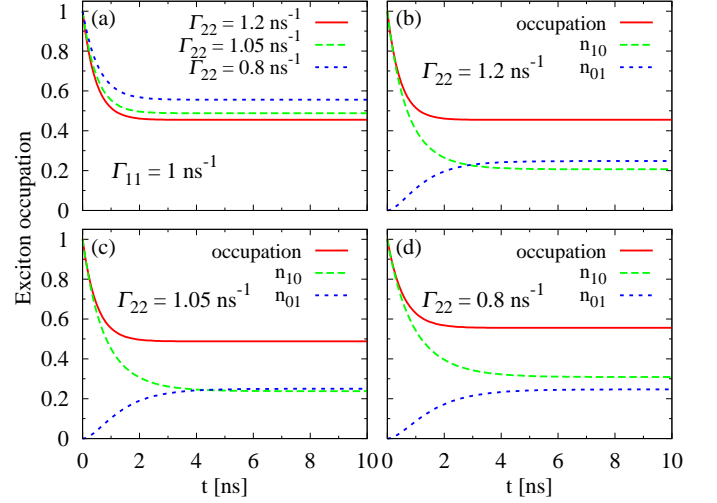


FIG. 2. (Color online) (a) Exciton occupation (red solid line) for a pair of decoupled ($V = 0$) QDs with identical transition energies ($\Delta = 0$) but with non-identical values of the spontaneous recombination rates ($\Gamma_{11} \neq \Gamma_{22}$). (b-d) The total exciton occupation (red solid line) and the occupations of the individual dots (green and blue dashed lines) for the three cases shown in (a). The value of $\Gamma_{11} = 1 \text{ ns}^{-1}$ is the same for all the graphs in this figure.

ally bigger than the lower one³⁶. The geometry and the structure of the QDs is reflected in the carrier wave functions and thus in the interband dipole moments. According to Eq. (5), this leads to different spontaneous decay rates for the two QDs forming the investigated system. The dipoles corresponding to the upper and lower QD may differ in amplitude and, if the hole states in the two structures have different light-hole admixtures, also in orientation (see Appendix).

The equation of motion describing the evolution of a system of two energetically identical ($\Delta = 0$) and uncoupled ($V = 0$) QDs interacting only with the radiation reservoir is described by Eq. (3) with $\mathcal{L}_{\text{ph}} = 0$ and \mathcal{L}_{rad} given by Eq. (4) with $\sigma_{\pm}^{\alpha}(t) = \sigma_{\pm}^{\alpha}$. It is known that in three-level open systems of this kind, non-radiating superposition states occur under certain conditions^{37–40}. In our case, a non-trivial (different than the ground state $|00\rangle\langle 00|$) stationary solution to the open system evolution equation, corresponding to the spontaneously formed, stable, delocalized dark state discussed above, exists only for $\Gamma_{12} = \sqrt{\Gamma_1 \Gamma_2}$, i.e., for parallel dipole moments [Eq. (5)] (such that $\hat{\mathbf{d}}_1 = \hat{\mathbf{d}}_2$ up to a phase factor). For dipoles that are parallel but have different amplitudes, the evolution is similar to the case of identical systems, i.e., coupling to photon surrounding leads to excitation transfer and occupation trapping. As can be seen in Fig. 2, the fraction of trapped exciton occupation depends on the values of the single dot decay rates and stabilizes at the level $\Gamma_{11}/(\Gamma_{11} + \Gamma_{22})$.

As in the case of identical QDs, the suppression of the exciton decay is due to the existence of a dark state

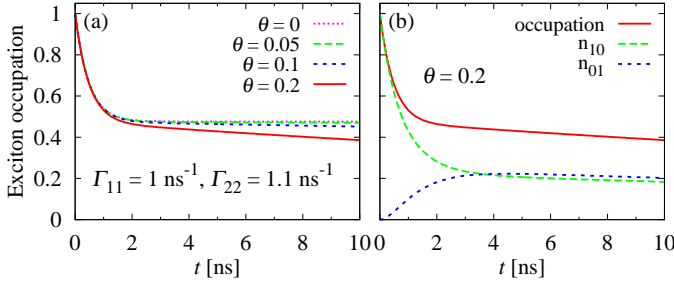


FIG. 3. Exciton occupation of a pair of uncoupled ($V = 0$) QDs with identical transition energies ($\Delta = 0$) and different spontaneous recombination rates ($\Gamma_{11} \neq \Gamma_{22}$) for a few values of the angle θ between the dipole moments. The values of Γ_{11} and Γ_{22} shown in Fig. (a) are valid for both figures.

which, for $\Gamma_{11} \neq \Gamma_{22}$, is not strictly anti-symmetric,

$$|\text{dark}\rangle = \frac{\sqrt{\Gamma_{11}}|10\rangle - \sqrt{\Gamma_{22}}|01\rangle}{\sqrt{\Gamma_{11} + \Gamma_{22}}}. \quad (7)$$

Due to unequal contribution from the single-exciton states to the dark state (7) the final occupation of the dots is non-symmetric, either, and equals

$$n_{10} = \left(\frac{\Gamma_{11}}{\Gamma_{11} + \Gamma_{22}} \right)^2 \quad \text{and} \quad n_{01} = \frac{\Gamma_{11}\Gamma_{22}}{(\Gamma_{11} + \Gamma_{22})^2},$$

respectively. Different dipole moments allow one to achieve different final situations. In the trapped state, the occupation of the initially excited dot may be lower [Figs. 2(b) and 2(c)] or higher [Fig. 2(d)] than that of the initially empty dot.

Another factor that influences the interband dipole moments is the light-hole admixture. If this admixture is different for the two dots then the dipole moments corresponding to the QDs forming the QDM or DQD become non-parallel (see Appendix). This means that the off-diagonal decay rate $\Gamma_{12} = \sqrt{\Gamma_{11}\Gamma_{22}}(1 - \theta^2/2) \neq \sqrt{\Gamma_{11}\Gamma_{22}}$, where θ is the angle between the interband dipole moments of the two dots [see Eq. (A.2)]. Consequently, the stationary solution to Eq. (4) does not exist and quenching of the final exciton occupation is observed. The values of θ are determined by the light hole admixture and typically are on the order of 0.01⁴¹. However, as can be seen in Fig. 3, even for much larger values of the angle between the dipoles, quenching of the occupation is weak. Although the system loses its coherence at long times, the character of the evolution remains the same as in the case of parallel dipoles on time scales much longer than the nominal exciton lifetime, i.e., initially excitation transfer between the dots takes place until the occupation rate n_{10}/n_{01} close to that defined by the decay rates Γ_{11} and Γ_{22} is reached and, then the impact of hole subband mixing is manifested as a slow and equal decay of occupations [Fig. 3(b)].

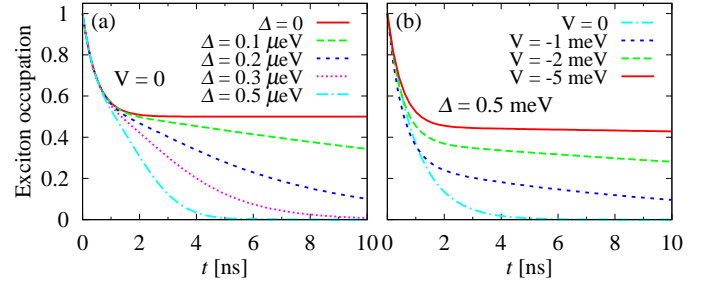


FIG. 4. (a) The impact of the energy mismatch on exciton occupation of a pair of uncoupled QDs. (b) Exciton occupation of a technologically realistic QDM for a few values of coupling between the emitters ($\Gamma_{11} = \Gamma_{22} = 1 \text{ ns}^{-1}$).

C. The role of the energy mismatch and coupling between the dots

In spite of rapid technological progress, manufacturing of DQDs or QDMs with identical fundamental transition energies is still not feasible. As can be seen in Fig. 4(a), for the realistic case of non-zero energy mismatch, the effect of trapping the system in an occupied and optically inactive state is destroyed. Already for the energy splitting on the order of tens of μeV quenching of the final occupation is observed (the relevant energy scale is the transition energy line width $\hbar\Gamma = 1.7 \mu\text{eV}$). QDs constituting such an inhomogeneous double dot systems interact with disjoint energy ranges of the electromagnetic field which destroys the collective character of coupling to photon modes. The energy mismatch of the dots slows the decay of the superradiant state and induces emission from the subradiant one²⁸. Due to the lack of a stable exciton state in which the system might be trapped the VIC effect in inhomogeneous QDMs is destroyed.

Initially, the character of the evolution of an exciton occupation of the inhomogeneous pairs of QDs does not differ considerably from the corresponding case of a pair of identical dots. Until $t \sim \hbar/(2\Delta)$, the coupling to photon modes maintains its collective character and excitation transfer from the initially occupied QD to the initially empty one takes place. Later, due to the emission from the subradiant as well as from the superradiant state, occupations of both dots decay²⁷.

If the distance between the QDs is sufficiently small coupling between the systems (Förster or tunneling) becomes effective and affects the evolution of carriers confined in the structure. Since sub- and superradiant states are eigenstates of the coupling part of the Hamiltonian [Eq.(2)] separated by the energy $2V$, sufficiently strong interaction between the dots rebuilds the collective character of the interaction even in structures with technologically realistic energy mismatches on the order of 1 meV^{19,28}. This also enables the VIC effect in inhomogeneous DQDs to be rebuilt. As can be seen in Fig. 4(b), for $V \gg \Delta$, a transition from a localized initial single-exciton state to a nearly stable state is possible for a system with

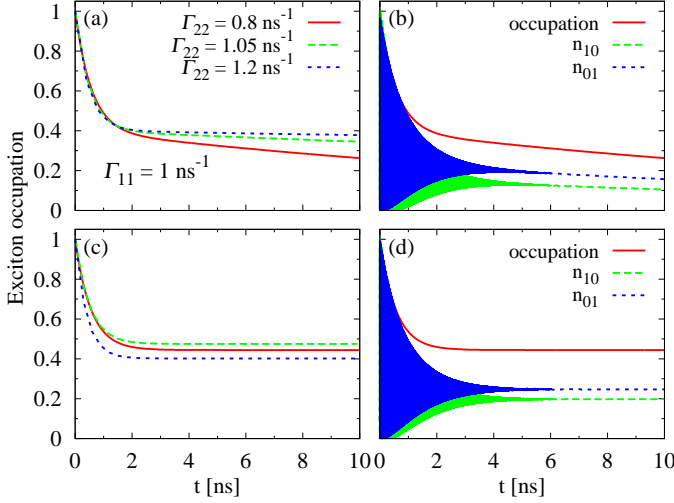


FIG. 5. Exciton occupation of a pair of technologically realistic QDs. (a) Total exciton occupation for $\Delta = 1$ meV, $V = -5$ meV, $\Gamma_{11} = 1$ ns $^{-1}$, and for a few values of Γ_{22} . (b) The total occupation and the occupations of the individual dots for the last case shown in (a). (c) Exciton occupation for three sets of parameters stabilizing the occupation trapping. Red solid line: $\Delta = 0.5$ meV, $V = -4.47$ meV, $\Gamma_{11} = 0.8$ ns $^{-1}$, $\Gamma_{22} = 1$ ns $^{-1}$. Green dashed line: $\Delta = 0.5$ meV, $V = -9.99$ meV, $\Gamma_{11} = 0.95$ ns $^{-1}$, $\Gamma_{22} = 1.05$ ns $^{-1}$. Blue dotted line: $\Delta = 1$ meV, $V = -5$ meV, $\Gamma_{11} = 1$ ns $^{-1}$, $\Gamma_{22} = 1.49$ ns $^{-1}$. (d) The total occupation and the occupations of the individual dots corresponding to the red line in (c).

a technologically achievable energy mismatch. Although full stabilization of the VIC effect is impossible for non-identical dots and quenching of the exciton occupation always takes place sufficiently strong coupling between the dots considerably reduces the decay of the trapped state. For a weaker coupling between the dots, the exciton occupation decay is faster but still reduced compared to the system of uncoupled QDs. In contrast to identical dots, the two localized states have different contributions from the from sub- and superradiant states. This results in a different degree of trapping depending on the choice of the initially occupied state²⁷.

D. Interplay of energy mismatch, coupling between the dots and non-uniform dipoles

For technologically realistic DQDs and QDMs, the fundamental energy mismatch of the two QDs forming the system is on the order of milli-electron-Volts, the dipole moments differ slightly between the dots and the systems are coupled with one another via Förster or tunneling coupling. The evolution of such systems, for parallel dipole moments, is shown in Fig. 5. In Fig. 5(a), the dynamics of a system strongly stabilized by a coupling between the dots is presented for a few values of the decay rates. As can be seen, the rate of occupa-

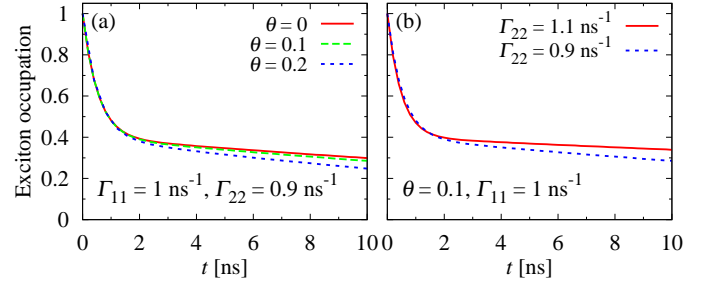


FIG. 6. Exciton occupation of a pair of non-identical ($\Delta = 1$ meV, $\Gamma_{11} \neq \Gamma_{22}$) and coupled ($V = -5$ meV) QDs for a few values of θ (a) and for two values of Γ_{22} (b).

tion decay depends on the choice of the two single-dot decay rate parameters. In such a system, the coherent excitation transfer between the dots takes place on time scales similar to the previously discussed cases. However, the initial state is now a superposition of non-degenerate system eigenstates, which leads to fast oscillations of the exciton occupation between the two dots [Fig. 5(b)].

In the present general case, the spontaneously formed coherence and the trapped occupation can again be fully stabilized by an appropriate choice of parameters in a system with parallel dipoles. The single-exciton eigenstates of the system Hamiltonian (1) are

$$|\Psi_1\rangle = \cos\left(\frac{\phi}{2}\right) |10\rangle + \sin\left(\frac{\phi}{2}\right) |01\rangle, \quad (8a)$$

$$|\Psi_2\rangle = -\sin\left(\frac{\phi}{2}\right) |10\rangle + \cos\left(\frac{\phi}{2}\right) |01\rangle, \quad (8b)$$

where $\tan(\phi) = V/\Delta$ and $\pi/2 \leq \phi < \pi/2$. The corresponding eigenenergies will be denoted by E_1, E_2 . If the coupling between the single exciton states satisfies the relation

$$V = -\frac{2\Delta\sqrt{\Gamma_{11}\Gamma_{22}}}{|\Gamma_{22} - \Gamma_{11}|} \quad (9)$$

then one of the eigenstates [Eqs. (8a) and (8b)] corresponds to the dark state (7). In such case, the evolution of a realistic system also leads to occupation trapping in a decoherence-resistant state [Fig. 5(c)] at the occupation $\Gamma_{11}/(\Gamma_{11} + \Gamma_{22})$. As can be seen from Eq. (9), non-equal values of the spontaneous decay rate for the two dots open a possibility to stabilize the evolution of the system for wide range of parameters. As for a system of identical dots, the occupations of single dots also stabilizes, but again initial fast oscillations due to contribution from two energy eigenstates are observed [Fig. 5(d)].

For the non-parallel dipole moments, i.e., for $\theta \neq 0$, the effect of occupation trapping is in principle destroyed but for strongly coupled dots, the decay is very weak. For the interesting time scale on the order of ns the impact of non-parallel dipoles becomes visible only for the values of θ that exceed the realistic ones by an order of magnitude⁴¹ (Fig. 6).

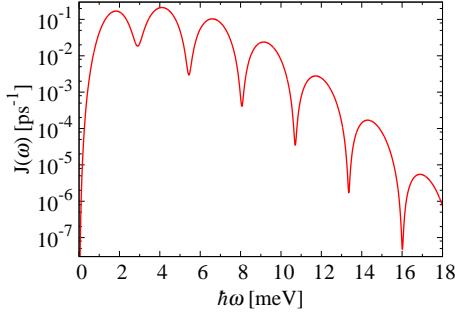


FIG. 7. (Color online) The phonon spectral density for $D = 8$ nm.

E. The role of lattice dynamics

Spontaneous emission from a system of QDs is affected by phonon dynamics^{31,42}. Coupling between the QDs and lattice vibrations induces excitation transfer between the two single exciton eigenstates [Eq. (8a) and (8b)]. For a pair of identical QDs ($\phi = \pm\pi/2$), these eigenstates exactly coincide with the bright (superradiant) and dark (subradiant) states $|+\rangle$ and $|-\rangle$ defined in Sec. IV A. If the dots are non-identical, there is no perfect correspondence between these two pairs of states but, for non-zero coupling, still one of them is brighter and the other is darker. As we have shown previously⁴², the phonon-induced redistribution of single exciton occupations among these two states strongly affects spontaneous emission in a temperature-dependent way. For the system of vertically stacked dots analyzed in this paper, the amplitudes of both tunneling and Förster couplings are negative, so that $\phi < 0$. In this case, the darker eigenstate has a higher energy and will be affected by relaxation even at low temperatures. As we show below, phonon dynamics indeed breaks the relative stability of the darker state and leads to considerably accelerated decay of the excitonic occupation, except for special parameter choices.

While, in general, non-Markovian effects may be important in the carrier-phonon dynamics that affects spontaneous emission⁴², the phonon-related effects to be discussed below can be understood within a Markovian picture of transitions between energy eigenstates. The corresponding rate for a transition between the eigenstates $|\Psi_i\rangle$ and $|\Psi_j\rangle$ is $\gamma_{i \rightarrow j} = 2\pi \sin^2 \theta J(|\omega_{ij}|) [n(\omega_{ij}) + 1]$, where $i, j = 1, 2$, $\omega_{ij} = (E_j - E_i)/\hbar$ and the spectral density is defined as

$$J(\omega) = \sum_{\mathbf{q}} |f_{\mathbf{q}}|^2 \sin^2 \frac{k_z D}{2} \delta(\omega - \omega_{\mathbf{q}}).$$

The spectral density for the inter-dot spacing $D = 8$ nm is plotted in Fig. 7. Apart from the usual cutoff at frequencies larger than \bar{l}/c due to the restriction on the momentum non-conservation $\Delta(\hbar q) \lesssim \hbar/\bar{l}$, where \bar{l} is the average dot size, it is characterized by the oscillations

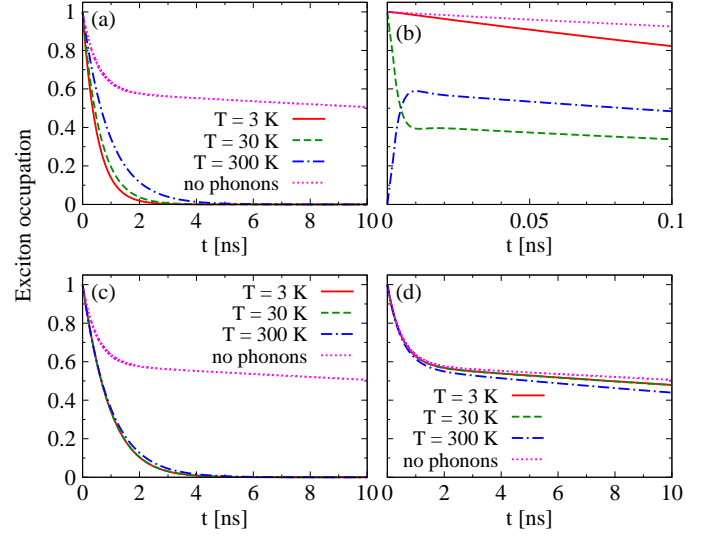


FIG. 8. Phonon impact on vacuum-induced coherence in a pair of QDs with a fixed V/Δ ratio (corresponding to $\phi = -1.4$): the comparison of the total exciton occupation in a system coupled to phonons and without phonons. (a) $\Omega = 4.0$ meV; (b) short-time section of (a) with solid (red) line representing the total exciton occupation, dotted (magenta) line corresponding to the total occupation without phonons and the dashed (green) and dash-dotted (blue) lines showing the occupations of the two dots; (c) $\Omega = 8.07$ meV (corresponding to the 3rd minimum of the spectral density); (d) $\Omega = 13.36$ meV (5th minimum of the spectral density).

with the period $\Delta\omega = 2\pi c/D$ which result from the double dot structure of the system⁴².

The phonon-related effects on the spontaneous buildup of coherence is shown in Fig. 8. Here we keep the mixing angle ϕ constant (there is, a constant ratio V/Δ) and use the energy splitting $\hbar\Omega = E_1 - E_2 = 2\sqrt{\Delta^2 + V^2}$ as a parameter. In Fig. 8(a) we plot the evolution of the total exciton occupation for $\hbar\Omega = 4.0$ meV, where the spectral density is relatively large, corresponding to phonon transition rates on the order of 1 ps^{-1} . One can see here that indeed the phonon-induced relaxation suppresses the vacuum-induced coherence, which is manifested by the rapid decay of the excitonic occupation. The role of phonons in this strong change of the occupation dynamics is clear in Fig. 8(b), where we show the first 100 ps of the same evolution. A very fast phonon-induced redistribution of occupations of the two dots (shown in green dashed and blue dash-dotted lines) takes place on a picosecond time scale after which the radiative effects are completely dominated by the phonon-induced thermalization which, at low temperatures, forces the system to stay in the bright state $|\Psi_2\rangle$. The detrimental effect of carrier-phonon coupling can only be avoided if the phonon-induced occupation dynamics is made slow compared to the spontaneous emission. This can be achieved by using the oscillating form of the phonon spectral density (see Fig. 7). As can be seen in Fig. 8(c,d), If choosing

the energy splitting $\hbar\Omega$ such that it corresponds to the 3rd minimum of the spectral density has little positive effect but for $\hbar\Omega$ in the 5th minimum, the phonon effects become very weak and the long living tail of the excitonic occupation is restored.

An interesting additional effect can be seen if one compares Figs. 8(a) and 8(d): If the phonon effects are strong then increasing the temperature slows down the occupation decay. However, for weak phonon influence the temperature dependence is opposite. This can be explained by noting that in the presence of fast phonon-induced redistribution of single exciton occupations, the occupation of these two states remains in quasi-equilibrium, which means that the occupation of the higher energy, darker state increases as the temperature grows. On the contrary, if the phonon-induced dynamics is slow the system state is almost unperturbed and close to the spontaneously formed dark superposition. Phonons lead to transitions out of this stable state with intensity growing with temperature.

V. CONCLUSIONS

We have studied the formation of vacuum-induced coherence and the associated long-living trapped excitonic population in a pair of vertically stacked semiconductor QDs. We focused on the features that distinguish QD systems from natural atoms: the mismatch of transition energies, coupling, possibly non-identical dipole moments for the optical transition, and strong interactions with the phonon environment.

We have shown that the VIC effect is very sensitive to the inhomogeneity of the QDs. Already for the fundamental transition energy mismatch on the order of the emission line width, the exciton occupation is quenched. However, the destructive effect of the energy inhomogeneity can be strongly reduced by coupling between the dots. While for dots with identical magnitudes of the interband dipole moments full stabilization of the spontaneously formed coherence can only be achieved in the limit of infinite coupling, in pairs of QDs with different interband dipoles it is possible to adjust the energy mismatch, the coupling between the QDs, and the dipole moments in such a way that a perfectly stable state forms in the spontaneous emission process and a fraction of the initial excitonic population attains a formally infinite life time. The non-parallel orientation of the interband dipoles, that may be caused by heavy-light hole mixing leads to negligibly weak effects in realistic structures. While carrier-phonon coupling typically destroys the vacuum induced coherence on picosecond time scales, it can be overcome by appropriately selecting the energy splitting between the single exciton states.

These results show that the VIC effect can be observed in realistic systems with energy splitting on the order of milli-electron-Volts provided that the system parameters (interband dipoles, coupling and energy mismatch) can

be controlled with sufficient flexibility. This seems to be possible by appropriately designing the system on the manufacturing stage and then employing the dependence of various parameters on external fields (e.g. via Stark effect or modification of electron-hole wave function overlap).

Let us note, finally, that the major experimentally detectable consequence of the appearance of vacuum-induced coherence in the double dot system is the long-living tail in the exciton occupation (or in luminescence intensity). Since this effect is of considerable amplitude and evolves on long, nanosecond time scales it should be relatively easily detectable with time-resolved luminescence or pump probe spectroscopy.

ACKNOWLEDGMENTS

A. S. acknowledges support within a “Młoda Kadra 2015 Plus” project, co-financed by the Polish Ministry of Science and Higher Education (MNiSW) and the European Union within the European Social Fund, and within a scholarship for outstanding young scientists granted by the Polish MNiSW.

Appendix: Interband dipole moments and subband mixing

In this appendix, we discuss the effect of light hole admixture on the non-parallel alignment of the interband dipoles for (nominally) heavy hole transitions.

Within the 4-band Luttinger model⁴³, the electron and hole wave functions are

$$\begin{aligned}\Psi_h^{(\alpha)}(\mathbf{r}, s) &= \sum_{\lambda} u_{\lambda}(\mathbf{r}, s) \varphi_{h\lambda}^{(\alpha)}(\mathbf{r}) \\ \Psi_e^{(\alpha)}(\mathbf{r}, s) &= u_{c\frac{1}{2}}(\mathbf{r}, s) \varphi_e^{(\alpha)}(\mathbf{r}),\end{aligned}$$

where $\alpha = 1, 2$ refers to a higher or lower QD, respectively, u_{λ} is a Bloch function for the valence subband λ (heavy holes: $\lambda = \pm 3/2$, light holes: $\lambda = \pm 1/2$), \mathbf{r} is the space coordinate, s denotes spin, $u_{c\frac{1}{2}}$ is an electron Bloch function with a fixed spin $s = 1/2$ (for definiteness) and $\varphi_{e/h}^{(\alpha)}$ refer to electron and hole envelope functions, respectively.

The matrix element of the interband dipole moment for the α th QD is

$$\mathbf{d}_{\alpha} = \sum_s \int d^3r \Psi_h^{(\alpha)}(\mathbf{r}, s) e \mathbf{r} \Psi_e^{(\alpha)}(\mathbf{r}, s).$$

To calculate the above integral we sum over unit cells (labeled by \mathbf{R}) and integrate over one unit cell ($\boldsymbol{\xi}$ labels the position within the cell). The envelope functions vary slowly which allows us to assume that they are constant over one unit cell, $\varphi_{e/h}(\mathbf{R} + \boldsymbol{\xi}) \approx \varphi_{e/h}(\mathbf{R})$. The Bloch

functions are periodic, $u(\mathbf{R} + \boldsymbol{\xi}, s) = u(\mathbf{R}, s)$, and orthogonal for different bands. As a result, we can write⁴⁴

$$\begin{aligned} \mathbf{d}_\alpha &= \frac{1}{v} \sum_{s, \lambda} \int_{u.c.} d^3 \mathbf{R} \int d^3 \boldsymbol{\xi} \\ &\quad \times u_\lambda(\boldsymbol{\xi}, s) \varphi_{h\lambda}^{(\alpha)}(\mathbf{R}) e(\mathbf{R} + \boldsymbol{\xi}) u_{c\frac{1}{2}}(\boldsymbol{\xi}, s) \varphi_e^{(\alpha)}(\mathbf{R}) \\ &= \sum_\lambda a_\lambda^{(\alpha)} \mathbf{d}_{\lambda, \frac{1}{2}}. \end{aligned}$$

Here $\mathbf{d}_{\lambda, \frac{1}{2}}$ is the bulk interband dipole moment,

$$\mathbf{d}_{\lambda, \frac{1}{2}} = \frac{1}{v} \sum_s \int_{u.c.} d^3 \boldsymbol{\xi} u_\lambda(\boldsymbol{\xi}, s) e \boldsymbol{\xi} u_{c\frac{1}{2}}(\boldsymbol{\xi}, s),$$

v is the unit cell volume,

$$a_\lambda^{(\alpha)} = \int d^3 \mathbf{R} \varphi_{h\lambda}^{(\alpha)}(\mathbf{R}) \varphi_e^{(\alpha)}(\mathbf{R})$$

is the envelop function overlap integral, and we have replaced the summation over unit cells with integration over \mathbf{R} .

We are investigating bright heavy hole excitons, hence $a_{-3/2}^{(\alpha)} \sim 1$ and the other coefficients $a_\lambda^{(\alpha)}$ are much smaller. The non-vanishing bulk dipole moment matrix elements involving the spin-1/2 electron state are^{44,45}

$$\begin{aligned} \mathbf{d}_{-\frac{3}{2}, \frac{1}{2}} &= -\sqrt{3} \mathbf{d}_{-\frac{1}{2}, \frac{1}{2}}^* = \frac{1}{\sqrt{2}} d_0 \begin{pmatrix} -1 \\ i \\ 0 \end{pmatrix}; \\ \mathbf{d}_{\frac{1}{2}, \frac{1}{2}} &= \sqrt{\frac{2}{3}} d_0 \begin{pmatrix} 0 \\ 0 \\ 1 \end{pmatrix}. \end{aligned}$$

Because the wave functions differ for the two QDs, the values of the heavy hole overlap integrals $a_{-\frac{3}{2}}^{(\alpha)}$ may vary.

Since, to the leading order,

$$\begin{aligned} |\mathbf{d}_\alpha| &= |d_0| \left(\left| a_{-\frac{3}{2}}^{(\alpha)} \right|^2 + \frac{2}{3} \left| a_{-\frac{1}{2}}^{(\alpha)} \right|^2 + \frac{1}{3} \left| a_{\frac{1}{2}}^{(\alpha)} \right|^2 \right)^{\frac{1}{2}} \\ &\approx \left| a_{-\frac{3}{2}}^{(\alpha)} \right| d_0 \left(1 + \frac{2 \left| a_{-\frac{1}{2}}^{(\alpha)} \right|^2 + \left| a_{\frac{1}{2}}^{(\alpha)} \right|^2}{6 \left| a_{-\frac{3}{2}}^{(\alpha)} \right|^2} \right), \end{aligned}$$

the difference of the overlap integrals leads to different magnitudes of the dipole moments $|\mathbf{d}_\alpha|$, $\alpha = 1, 2$. Moreover, one has

$$\mathbf{d}_1 \cdot \mathbf{d}_2^* = a_{-\frac{3}{2}}^{(1)} a_{-\frac{3}{2}}^{(2)*} |d_0|^2 \left(1 + \frac{2 a_{-\frac{1}{2}}^{(1)} a_{-\frac{1}{2}}^{(2)*}}{3 a_{-\frac{3}{2}}^{(1)} a_{-\frac{3}{2}}^{(2)*}} + \frac{1 a_{\frac{1}{2}}^{(1)} a_{\frac{1}{2}}^{(2)*}}{3 a_{-\frac{3}{2}}^{(1)} a_{-\frac{3}{2}}^{(2)*}} \right).$$

Hence,

$$\begin{aligned} |\hat{\mathbf{d}}_1 \cdot \hat{\mathbf{d}}_2^*| &= \frac{|\mathbf{d}_1 \cdot \mathbf{d}_2^*|}{|\mathbf{d}_1| |\mathbf{d}_2|} \\ &\approx 1 - \frac{1}{3} \left| \frac{a_{-\frac{1}{2}}^{(1)}}{a_{-\frac{3}{2}}^{(1)}} - \frac{a_{-\frac{1}{2}}^{(2)}}{a_{-\frac{3}{2}}^{(2)}} \right|^2 - \frac{1}{6} \left| \frac{a_{\frac{1}{2}}^{(1)}}{a_{-\frac{3}{2}}^{(1)}} - \frac{a_{\frac{1}{2}}^{(2)}}{a_{-\frac{3}{2}}^{(2)}} \right|^2. \quad (\text{A.1}) \end{aligned}$$

Thus, if the light hole admixture is different for the two dots,

$$\frac{a_{\pm\frac{1}{2}}^{(1)}}{a_{-\frac{3}{2}}^{(1)}} \neq \frac{a_{\pm\frac{1}{2}}^{(2)}}{a_{-\frac{3}{2}}^{(2)}}$$

then $\hat{\mathbf{d}}_1 \cdot \hat{\mathbf{d}}_2^* \neq 1$, that is, the dipoles are non-parallel.

As the subband mixing is typically small in self-assembled structures the angle θ between the dipole moments is small. Therefore, one can write

$$\hat{\mathbf{d}}_1 \cdot \hat{\mathbf{d}}_2^* = e^{i\eta} \cos \theta \approx e^{i\eta} \left(1 - \frac{1}{2} \theta^2 \right), \quad (\text{A.2})$$

where η is an irrelevant phase. Comparing Eqs. (A.1) and (A.2) one gets

$$\theta = \left(\frac{2}{3} \left| \frac{a_{-\frac{1}{2}}^{(1)}}{a_{-\frac{3}{2}}^{(1)}} - \frac{a_{-\frac{1}{2}}^{(2)}}{a_{-\frac{3}{2}}^{(2)}} \right|^2 + \frac{1}{3} \left| \frac{a_{\frac{1}{2}}^{(1)}}{a_{-\frac{3}{2}}^{(1)}} - \frac{a_{\frac{1}{2}}^{(2)}}{a_{-\frac{3}{2}}^{(2)}} \right|^2 \right)^{\frac{1}{2}}.$$

* anna.sitek@pwr.wroc.pl

† pawel.machnikowski@pwr.wroc.pl

¹ B. W. Lovett, J. H. Reina, A. Nazir, and G. A. D. Briggs, Phys. Rev. B **68**, 205319 (2003).

² J. Danckwerts, K. J. Ahn, J. Förstner, and A. Knorr, Phys. Rev. B **73**, 165318 (2006).

³ G. W. Bryant, Phys. Rev. B **47**, 1683 (1993).

⁴ A. Schliwa, O. Stier, R. Heitz, M. Grundmann, and D. Bimberg, Phys. Stat. Sol. (b) **224**, 405 (2001).

⁵ B. Szafran, S. Bednarek, and J. Adamowski, Phys. Rev. B

64, 125301 (2001).

⁶ B. Szafran, Acta Phys. Polon. A **114**, 1013 (2008).

⁷ E. Pazy, I. D'Amico, P. Zanardi, and F. Rossi, Phys. Rev. B **64**, 195320 (2001).

⁸ T. Unold, K. Mueller, C. Lienau, T. Elsaesser, and A. D. Wieck, Phys. Rev. Lett. **94**, 137404 (2005).

⁹ E. Biolatti, R. C. Iotti, P. Zanardi, and F. Rossi, Phys. Rev. Lett. **85**, 5647 (2000).

¹⁰ F. Troiani, E. Molinari, and U. Hohenester, Phys. Rev. Lett. **90**, 206802 (2003).

- ¹¹ A. Nazir, B. W. Lovett, S. D. Barrett, T. P. Spiller, and G. A. D. Briggs, *Phys. Rev. Lett.* **93**, 150502 (2004).
- ¹² E. M. Gauger, A. Nazir, S. C. Benjamin, T. M. Stace, and B. W. Lovett, *New J. Phys.* **10**, 073016 (2008).
- ¹³ O. Gywat, G. Burkard, and D. Loss, *Phys. Rev. B* **65**, 205329 (2002).
- ¹⁴ J. E. Rolon and S. E. Ulloa, *Phys. Rev. B* **82**, 115307 (2010).
- ¹⁵ M. Goryca, T. Kazimierzuk, M. Nawrocki, A. Golnik, J. A. Gaj, P. Kossacki, P. Wojnar, and G. Karczewski, *Phys. Rev. Lett.* **103**, 087401 (2009).
- ¹⁶ S. Gustavsson, M. Studer, R. Leturcq, T. Ihn, K. Ensslin, D. C. Driscoll, and A. C. Gossard, *Phys. Rev. Lett.* **99**, 206804 (2007).
- ¹⁷ P. Borri, W. Langbein, U. Woggon, M. Schwab, M. Bayer, S. Fafard, Z. Wasilewski, and P. Hawrylak, *Phys. Rev. Lett.* **91**, 267401 (2003).
- ¹⁸ C. Bardot, M. Schwab, M. Bayer, S. Fafard, Z. Wasilewski, and P. Hawrylak, *Phys. Rev. B* **72**, 035314 (2005).
- ¹⁹ B. D. Gerardot, S. Strauf, M. J. A. de Dood, A. M. Bychkov, A. Badolato, K. Hennessy, E. L. Hu, D. Bouwmeester, and P. M. Petroff, *Phys. Rev. Lett.* **95**, 137403 (2005).
- ²⁰ R. H. Dicke, *Phys. Rev.* **93**, 99 (1954).
- ²¹ M. Scheibner, T. Schmidt, L. Worschech, A. Forchel, G. Bacher, T. Passow, and D. Hommel, *Nat. Phys.* **3**, 106 (2007).
- ²² N. S. Averkiev, M. M. Glazov, and A. N. Poddubnyi, *Zh. Eksp. Teor. Fiz.* **108**, 958 (2009), [*J. Exp. Theor. Phys.* **108**, 836 (2009)].
- ²³ V. I. Yukalov and E. P. Yukalova, *Phys. Rev. B* **81**, 075308 (2010).
- ²⁴ M. Kozub, L. Pawicki, and P. Machnikowski, arXiv:1201.4059 (unpublished).
- ²⁵ G. S. Agarwal, *Quantum Statistical Theories of Spontaneous Emission and their Relation to Other Approaches*, Vol. 70 of *Springer tracts in modern physics*, G. Höhler (Ed.) (Springer, Berlin, 1974).
- ²⁶ M. Bayer, P. Hawrylak, K. Hinzer, S. Fafard, M. Korkusinski, Z. R. Wasilewski, O. Stern, and A. Forchel, *Science* **291**, 451 (2001).
- ²⁷ A. Sitek and P. Machnikowski, *Phys. Stat. Sol. (b)* **248**, 847 (2011).
- ²⁸ A. Sitek and P. Machnikowski, *Phys. Rev. B* **75**, 035328 (2007).
- ²⁹ A. Sitek and P. Machnikowski, *Phys. Rev. B* **80**, 115319 (2009).
- ³⁰ A. Sitek and P. Machnikowski, *Phys. Rev. B* **80**, 115301 (2009).
- ³¹ P. Machnikowski, K. Roszak, and A. Sitek, *Acta Phys. Polon. A* **116**, 818 (2009).
- ³² B. Szafran, T. Chwiej, F. M. Peeters, S. Bednarek, J. Adamowski, and B. Partoens, *Phys. Rev. B* **71**, 205316 (2005).
- ³³ K. Roszak and P. Machnikowski, *Phys. Rev. A* **73**, 022313 (2006), quant-ph/0507027.
- ³⁴ P. Machnikowski, *J. Phys: Conf. Ser.* **193**, 012136 (2009).
- ³⁵ W. Rudno-Rudzinski, R. Kudrawiec, P. Podemski, G. Sek, J. Misiewicz, A. Somers, R. Schwertberger, J. P. Reithmaier, and A. Forchel, *Appl. Phys. Lett.* **89**, 031908 (2006).
- ³⁶ R. Heitz, I. Mukhametzhanov, P. Chen, and A. Madhukar, *Phys. Rev. B* **58**, R10151 (1998).
- ³⁷ D. A. Cardimona, M. G. Raymer, and C. R. S. Jr, *J. Phys. B* **15**, 55 (1982).
- ³⁸ G. C. Hegerfeldt and M. B. Plenio, *Phys. Rev. A* **46**, 373 (1992).
- ³⁹ A. R. R. Carvalho, P. Milman, R. L. de Matos Filho, and L. Davidovich, *Phys. Rev. Lett.* **86**, 4988 (2001).
- ⁴⁰ M. M. Santos, F. O. Prado, H. S. Borges, A. M. Alcalde, J. M. Villas-Bôas, and E. I. Duzzioni, *Phys. Rev. A* **85**, 032323 (2012).
- ⁴¹ K. Gawarecki and P. Machnikowski, *Phys. Rev. B* **85**, 041305(R) (2012).
- ⁴² P. Karwat, A. Sitek, and P. Machnikowski, *Phys. Rev. B* **84**, 195315 (2011).
- ⁴³ J. M. Luttinger, *Phys. Rev.* **102**, 1030 (1956).
- ⁴⁴ H. Haug and S. W. Koch, *Quantum Theory of the Optical and Electronic Properties of Semiconductors* (World Scientific, Singapore, 2004).
- ⁴⁵ V. M. Axt, Ph.D. thesis, Rheinisch-Westfälische Technische Hochschule Aachen, 1994.